A possible concept for the day-time calibration and co-phasing of the adaptive M4 mirror at the E-ELT telescope

Briguglio, Runa, Pariani, Giorgio, Xompero, Marco, Riccardi, Armando, Tintori, Matteo, et al.

Runa Briguglio, Giorgio Pariani, Marco Xompero, Armando Riccardi, Matteo Tintori, Daniele Gallieni, Roberto Biasi, "A possible concept for the day-time calibration and co-phasing of the adaptive M4 mirror at the E-ELT telescope," Proc. SPIE 10703, Adaptive Optics Systems VI, 1070379 (18 July 2018); doi: 10.1117/12.2314460

SPIE.

Event: SPIE Astronomical Telescopes + Instrumentation, 2018, Austin, Texas, United States

A possible concept for the day-time calibration and co-phasing of the adaptive M4 mirror at the E-ELT telescope

Runa Briguglio[a], Giorgio Pariani[b], Marco Xompero[a], Armando Riccardi[a], Matteo Tintori[c], Daniele Gallieni[c], and Roberto Biasi[d]

[a]INAF Osservatorio Astrofisico Arcetri L. E. Fermi 5, 50125 Firenze Italy
[b]INAF Osservatorio Astronomico Brera, via E. Bianchi 46, 23807 Merate (LC) Italy
[c]ADS International
[c]Microgate

ABSTRACT

The M4 unit is the deformable mirror providing the E-ELT with adaptive correction of the atmospheric turbulence. The mirror is segmented into 6 petals which are actively shaped by more than 5000 voice-coil actuators. They are controlled in close loop with internal metrology through co-located capacitive position sensors. INAF is involved in the optical calibration and verification of the M4 unit and designed the laboratory optical testbed In this paper, we present a possible auxiliary setup for the mirror calibration once installed at the telescope. The concept implements an on-demand, day-time, optical re-calibration of the mirror, to ensure the years-long term, high accuracy, high precision stability of the internal metrology, beyond the already remarkable intrinsic electronic stability of the M4 unit. The setup exploits the two focii of the quasi-elliptical M3 to create an optical cavity, with the interferometer placed at a Nasmyth focal station of the ELT and a retroreflector (or fiber source) at the M3 short focus to measure the M4 in double (or single) pass. The full monitoring of the M4 optical area allows to: calibrate the actuator influence functions to compute the segments piston tip/tilt commands with high precision; retrieve the flattening command to correct from the low and high order features generated by thermo-mechanical and electrical drifts; compute the phasing command to correct for the segments differential alignment and piston within the requested WF accuracy. The system offers a fast and effective optical maintenance facility for the M4U, without requiring an additional test tower and the mount/dismount down-time of the unit. In this work, we summarize the optical layout and the flattening and segments co-phasing strategy.

Keywords: Adaptive Optics, Wavefront correctors, Deformable mirrors, Optical calibration, Laser Interferometry

1. INTRODUCTION: THE M4U

The European Extremely Large Telescope (E-ELT) will be the largest optical telescope on Earth. To exploit its resolving power, it will be a fully adaptive telescope, as it will be fitted with a wavefront corrector within its optical train. Such element is the quaternary mirror M4,[1] which is a deformable mirror of 2.5 m diameter, segmented into 6 petals and controlled by 5316 actuators. The mirror technology has been inherited by the LBT and VLT deformable secondary mirrors:[1] the optical surface is a thin glass shell (TS) *floating* in front of a reference body (RB) thanks to the magnetic force applied by voice coil actuators. The force is controlled in a local close loop, with the feedback of co-located capacitive sensor, measuring at high frequency the distance (*gap*) between the TS and the RB.

The design, manufacturing, integration and test of the unit is under the responsibility of AdOptica, an italian industrial consortium composed by Microgate and ADS. The Italian Institute for Astrophysic (INAF) has the role of supporting the challenging optical calibration and test of the deformable mirror, including the co-phasing of the 6 segments. Within this task, an optical test facility has been designed (the OTT, described in[2]), as long

Further author information:
Runa Briguglio: E-mail: runa@arcetri.astro.it, Telephone: +39 055 2752200

Adaptive Optics Systems VI, edited by Laird M. Close, Laura Schreiber, Dirk Schmidt, Proc. of SPIE Vol. 10703, 1070379 · © 2018 SPIE
CCC code: 0277-786X/18/$18 · doi: 10.1117/12.2314460

as the calibration procedure[3] and the associated error budget.[4] A dedicated numerical code[5] has been developed to simulate and assess the key-points of the procedure. The challenges of the optical calibration come from the very tight performance requirements, that may be summarized in the flattening and co-phasing (including stability) specification, as low as 20 nm RMS WF.

2. CO-PHASING STABILITY AT THE TELESCOPE

The optical measurement error budget indicates that the flattening and phasing stability are within the specification. This includes the measurement noise, the print-through from the OTT optics and the alignment residues. The long term stability of the phasing is a different element of the specification beyond the optical measurement. It involves, in facts, the long term stability of the M4 control electronics, namely the capacitive sensor components and the reference signal generators. Such aspects have been extensively assessed within the LBT and VLT deformable mirror projects. The novelty here is that M4 is segmented and each mirror segment has individual actuators and capacitive sensor electronics: the co-phasing stability implies therefore the differential stability of the reference signals amongst the segments, within the 3 years time scale specified in the requirement. The main point is that there exists no sufficient documentation nor experimental validation to assess such differential stability of the reference signals; we are forced to extrapolate the short term data (as provided by the manufacturer of the electronic components) to 3 years, so that our estimation of the co-phasing accuracy becomes a very upper limit of tens of nanometer, yet beyond specification.

2.1 Active correction

We identified a possible risk-mitigation strategy, based on the on-telescope, day-time measurement and correction of the phasing error with the optical feedback of the interferometer. The concept has been named NaPS (Nasmyth Phasing Sensor). The NaPS concept is based on the wavefront sensor (e.g., the interferometer) placed at the long focus of M3. The idea is to measure the M4U though M5 and M3, by means of the two focii of the quasi-elliptical M3 mirror. The optical scheme may be implemented both double-pass or single pass. In the double pass configuration a retroreflector (RR) is placed at the E-ELT intermediate focus to fold back the light on the same path toward the interferometer, while the single-pass option is fed by a fiber source at the short focus of M3, routed for the generation of the spherical reference signal, and a fiber-fed interferometer with the correction optics is placed at the Nasmyth focus. A similar concept based on an internal source has been also proposed[6] to serve as a common tool for the calibration of the E-ELT wavefront sensor units.

Supposing any possible movement of the E-ELT telescope optics, we can foreseen both the on-axis and off-axis configurations, the former with the RR (or fiber) placed in the center of the M4 hole, the latter with the RR (or fiber) placed at a side of the M4 hole. Actually, the on-axis design requires a deployment mechanism to place the RR (or fiber) at the center of the E-ELT focus, but no large movements of the telescope optics are required, except to compensate for RR (or fiber) deployment accuracy. The off-axis design considers the RR (or fiber) permanently installed in the M4 hole, but large movements of the telescope mirrors, especially M3, are necessary to recover the on-axis alignment between the RR and M3. According to our best knowledge about M3 positioning this solution can not be implemented. We will describe in more details the on-axis, double pass solution being the easiest to be implemented with a commercial interferometer.

3. THE NAPS

3.1 Optical design

In the on-axis, double pass solution the interferometer is placed at the Nasmyth platform of E-ELT and the retroreflector (RR) at E-ELT intermediate focus. To cope with air turbulence and freeze mechanical vibrations we are considering a Twymann-Green vibration insensitive interferometer.[7] The interferometer is equipped with a diverging lens to generate a F/15.7 beam, to feed M3. In a tentative design, the RR is placed on-axis about 400 mm above the E-ELT intermediate focus, to be inserted when needed without interfering with M4 itself. The concept is shown in Fig. 1. RR has a 375 mm radius of curvature, 110 mm clear aperture and has to be aspheric to compensate the departure of M3 from the elliptical shape. The theoretical residual WFE in double pass is negligible, below 5 nm RMS, but is ultimately limited on the manufacturing quality of the optics.

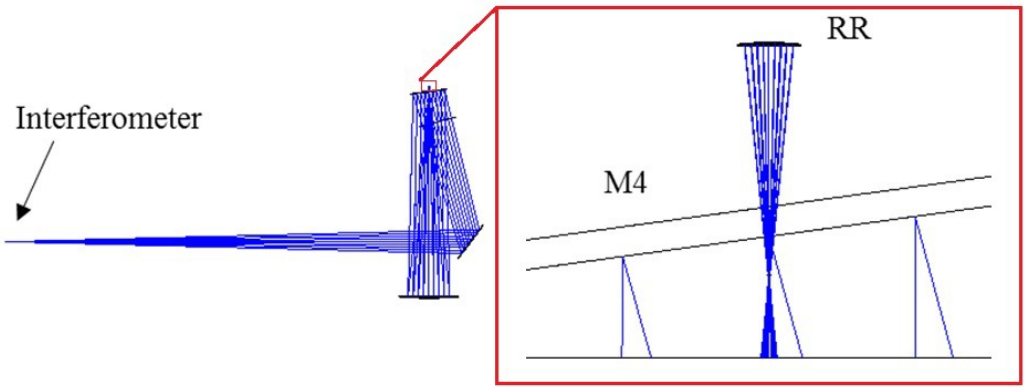

Figure 1. The double pass NaPS design. The interferometer is placed at the Nasmyth platform on the left. The beam is folded by M5, M4 and M3 and the cavity is closed at the telescope intermediate focus by a retro-reflecting optics.

3.2 Image quality and resolution

One of the main concerns in the double pass configuration is the quality of the pupil (i.e., the M4U image). In fact, there are virtually two M4 mirrors at different positions along the optical path that shall be in focus. Alternatively, we need to investigate if a phase blurring occurs when a slope is applied on the M4 surface. In fact, in the nominal configuration there are no retrace differences between the forward and backwards beams, with no degradation in the pupil resolution. On the contrary, if a slope is applied to M4, a ray originated on M4 in the first pass will hit M4 in the second pass at a certain distance, that shall be verified to be lower than the interferometer spatial resolution at the M4 level.

To do this, we placed the pupil on M4 in the first pass ($M4_1$) and calculated the position (x_2) and size (D_2) of the second pupil of M4 ($M4_2$) as respect to the first one. A slope s applied on $M4_1$ is amplified by the ratio of the pupil sizes $D_1/D_2 = 14$, and the beam originated on $M4_1$ hits $M4_2$ at a distance of $s \cdot x_2 = s \cdot 37m$. If we consider that the interferometer resolution is about 2 mm/pixel at the M4 level (2500mm/1200pixel), these means that we can tolerate WF slopes at the $M4_2$ level of about $2mm/37m = 54urad$ and at the $M4_1$ level of about $54urad/14 = 4urad$ without degradation of the M4 image. These corresponds to a maximum global WF tilt of about 10um (80 tilt fringes) to preserve the best image resolution, which is well enough to measure the low order modes of the mirror, or about 100nm WF over the inter-actuator distance when measuring the zonal IFs or the high order modal IFs. Larger slopes can be tolerated with a corresponding degradation of the image resolution, until information cross talks my take place between adjacent actuators, which in any case corresponds to a spatial resolution of 10-15 mm, or a global WF slope of 20-30urad.

3.3 Tolerances and sensitivities

Alignment tolerances in the deployment of the RR have been evaluated by misplacing it in any degree of freedom (DoF) and applying a compensation in 5 DoFs with M3, to restore the on-axis condition, and in tip/tilt with M4 and M5, to correct for the residual cavity tilt. All RR misplacements are compensated with a repositioning in the telescope mirrors, with no degradation on the nominal cavity WF if the movement is perfect. Accordingly, RR can be deployed with rough accuracy, since misplacements can be fully corrected. The final accuracy is only limited by the correction range and resolution of the E-ELT mirrors which may leave residuals in the cavity alignment compensation.

Fringe sensitivities were also evaluated. In fact, vibrations in the optical components are primarily responsible for the tilt and focus fringes in the interferogram. In plane displacements of the RR are the major contributors to tilt fringes, with a quite high sensitivity. In any case, we should remember that this effect is frozen by the dynamic interferometer we are considering, unless large vibrations at the MHz are present. Up to now we considered the effect of the RR only, a detailed modeling of the all elements is required to ultimately access this point.

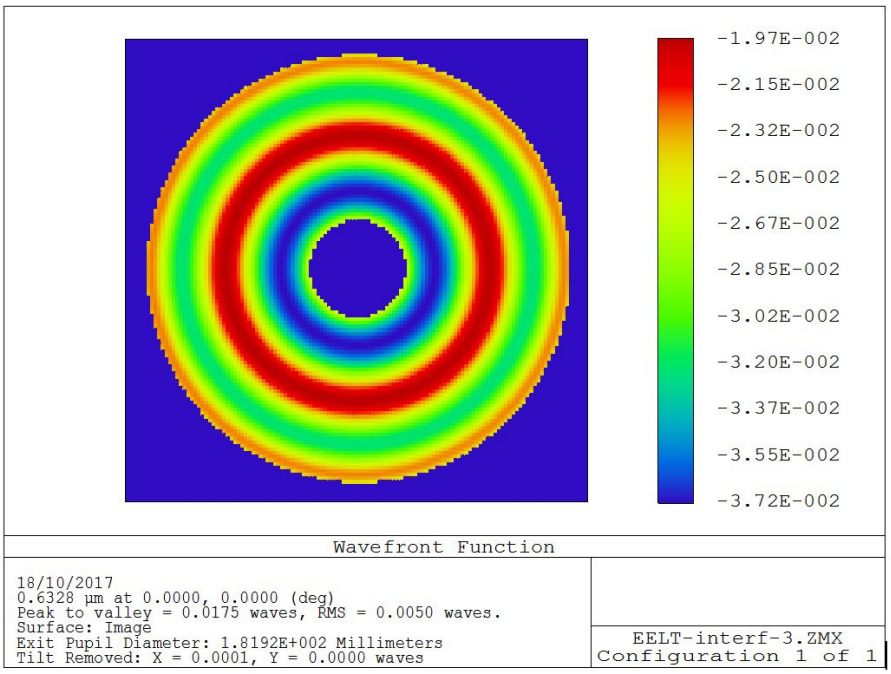

Figure 2. Expected aberration of the NaPS after re-aligning the E-ELT mirrors to recover deployment error of the RR.

RR DoF	fringe sensitivity	WFE 500 fringes (um RMS)
dx, dy	1.3 um/fringe	0.22 focus, astigmatism at 0.25% over tilt
dz	20 um/fringe	40 focus, second order focus at 0.5% over focus
tx, ty	3 urad/fringe	2 coma, at 3% over tilt

Table 1. Table of sensitivity for the NaPS.

Due to the optical setup, global tip/tilt, alignment focus and coma are unseen modes. Residual WFE due to long term drifts (e.g. thermal) after the initial cavity alignment can't be evaluated at present, but are not affecting the test accuracy when differential measurements are performed, as for the measurement of the IFs.

4. THE PHASING STRATEGY

The phasing of a deformable mirror consists in a segments vertical displacement produced via an actuator command. Such a command is not a unitary vector because of the spread of the actuator gains. As a consequence, the piston mode shall be optically calibrated, or equivalently, the actuators gain shall be measured to apply a pure optical piston.

4.1 Overview of the phasing procedure

We considered a phasing procedure based on the measurement of the mirror influence functions (IF) and the computation of the optical piston within the basis provided by the IF. The phasing command is then applied in close loop. The interferometer phase ambiguity does'nt affect the procedure as we expect that the capacitive sensor drift to be managed is much lower than the phase ambiguity. Such point is also a constraint on the mirror WFE before starting the phasing procedure. It follows that at any time the segments position is within the same lambda and the interferometer signals associated may be analytically post-processed to match such condition. The piston command is a pure vertical displacement so that is can be in principle produced by the actuators with zero fitting error (and zero force). However, the external edge of the optical surface is equipped with flexures to prevent lateral displacements. The stiffness of such membranes is very low for vertical movements, we expect the same some fitting error in the application of the piston command.

4.2 Measurement of the actuators and rigid body IF

The first step consists in the measurement of the IF. The measurement is based on the sequential application and sampling of the mirror modes at the fastest frame rate allowed by the interferometer. The sampling is performed with the push-pull technique, so that high frequency acquisition has the benefit of reducing the low frequency noise contribution such as air convection and vibrations. The optical piston is produced by a linear combination of all the mirror modes, so that in principle we need to sample and control the entire modal basis. In facts, only a subset of modes includes a significant piston contribution; in particular the modes in the range 0 to 10. The full modal basis is still requested, to compensate the offset added by the modes that produce a piston; it is also requested to correct the high orders introduced by the membranes when the vertical displacement is applied.
The sampling and post processing of the IF data deserve some more discussion. The flattening of a deformable, monolithic mirror does'nt include the correction of piston and alignment modes, in particular tip/tilt. In that case we are allowed to filter out piston and tip/tilt, both from the modal basis data and from the reference image to compute the flattening command. It follows that neither the tip/tilt noise from vibration nor the interferometer phase ambiguity have any impact on the flattening. The M4 is a segmented mirror so that the differential alignment amongst segments shall be corrected, so that we cannot simply filter piston and tip/tilt from the IF. These aspects will be addressed in the following.

4.2.1 Tip/tilt commands

Tip/tilt commands may be retrieved from the IF by mean of a dedicated processing even in presence of large vibration noise. The sampling and processing procedure may be summarized as follows. Let's consider the mirror modes matrix V_i of the i-th segment; the full, six segments modes matrix is a block diagonal

$$V = \begin{matrix} V_0 & 0 & ... \\ 0 & V_1 & ... \\ 0 & ... & V_5 \end{matrix}$$

We impose that the IF of the various segments are not collected together, i.e. one or more segments at a time are not acted while measuring the other(s). Each frame w (corresponding to the difference between two consecutive images according to the push-pull algorithm) may be re-organized pixel-wise as to group together the pixel associated with each segment. We obtain a $w* = [\omega_{acted}, \omega_{idle}]$, where ω_{acted} are the pixel associated with acted segments and ω_{idle} corresponds to un-acted segments. The ω_{idle} have not zero values because they sample the (differential noise) at the time of acquisition. We can then compute the frame-to-frame tip/tilt contribution from the ω_{idle}, evaluate the mean tilt coefficient amongst the un-acted segments and compute a syntetic tilt map to be subtracted from the ω_{acted}. In this way the IF data are corrected for the vibration tilt so that the signal measured on the WF map represents the optical tilt produced by the actuators for each mode. Such *tilt-detrending* procedure have been successfully implemented and tested during the optical calibration of the M4 Demonstration Prototype (M4DP) and the results are shown in.[8]

4.2.2 Piston commands

In order to correctly retrieve the optical piston, the actuator commands to measure the IF shall not exceed the interferometer phase ambiguity. If such condition is satisfied we have an a-priori information on the piston value within the frame; the phase ambiguity may be then solved using this information. The command amplitude shall then be as low as 20 to 50 nm RMS, so that a dedicated sampling strategy shall be investigated to guarantee a suitable SNR. We defined the following:

1. the first 10 modes (taken from the mirror modes matrix V) are sampled in push-pull with low command amplitude and robust averaging (25 frames/modes, e.g.);
2. the piston command is fitted from these data and a new command matrix V*=(P, V*1, V*2...) is created, where P is the optical piston command and the V*i are the modes in V after subtracting P.;

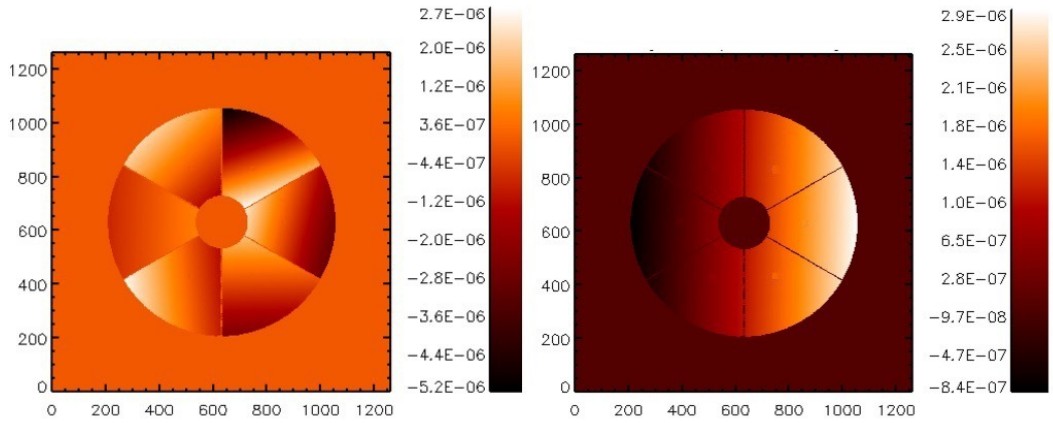

Figure 3. Simulated phase map of the M4 as measured by the NaPS after flattening, before (left) and after (right) the co-alignment and phasing. The residual tilt may be compensated by rotating the entire unit.

3. the mode P is sampled with low amplitude and very robust averaging, for instance 20 nm RMS and 100 frames;

4. the other modes in V* are sampled together with the rest of the modes matrix V.

The IF of the first mirror modes shall be measured with a low command amplitude, so that the signal will not exceed the interferometer phase ambiguity; the piston signal may be then retrieved with no distortion. Once the pure piston command has been calibrated, together with the piston-free command matrix, we may re-collect the IF with command amplitudes tuned separately for piston and high orders and achieve a suitable SNR for all of them.

4.3 Co-flattening and phasing

In the OTT, these two operations are kept separated (i.e. run sequentially) to avoid blending the phasing signal from local feature. In the NaPS, thanks to the global visibility of the M4, the shells flattening and phasing may be executed in principle in a single shot. We will prefer however to keep the two steps separately: in facts, because of the interferometry phase ambiguity, a piston-equalization algorithm shall be run in post processing on the frames. Such algorithm may produce artefacts if the WF on the shell islands has a large content of locally non zero signal. To this purpose, we will first run the individual shell flattening (all shells in a single step), that does'nt require any piston leveling, and then the cophasing on the perfectly flat shells. The flattening of course shall include the correction of the differential alignment, i.e. the shells tip/tilt.
Both flattening and phasing consist in the minimization of the current signal (in WFE, as measured by the interferometer) by the application of a proper actuator commands. The correction is therefore intrinsically limited by the actuator fitting error. For rigid body shapes (such as tip-tilt and piston) the fitting error is zero, apart from the static print-through given the external membranes holding the shells. The actuator commands is computed as $c_a = -Rw_i = -M^+ w_i$ where, $R = M^+$ is the pseudo inverse of the optical interaction matrix M and w_i is the current phasemap as measured by the interferometer. By definition, only the shapes within the M are applied, so that in order to perform both the flattening and co-phasing, M shall contain the influence functions of the mirror eigenmodes and of the rigid body shapes. This is however guaranteed by sampling the influence functions of all the modes in the V matrix as described above. V is in facts a command matrix collecting together (with no mutual cross-talk) the tip/tilt/piston-free mirror modes and the rigid body shapes.

4.4 Discussion on noise sources on co-phasing

Vibration noise is responsible for a global tip/tilt offset. Such term is well defined over the M4U area and may be fitted and subtracted to produce a zero-tilt image to measure the differential piston amongst the segments. Therefore, we will not consider the vibration noise in our analysis. Air convection is responsible for a moving

WF offset, as long as the air flows through the measuring beam. A differential piston signal is created when the WF average is different over the segments. We evaluated such offset by analyzing a set of noise data collected with the LBT adaptive secondary, both in the dome environment at LBTO (Mnt Graham, Arizona) and in the Arcetri test tower (ATT, Florence, Italy). In both cases the optical path is vertical, 15 m back and forth. We analyzed the datasets with the following procedure:

1. Each frame is fitted to estimate and subtract the global piston and tip/tilt;
2. the mirror area is divided into two islands to simulate two separated segments
3. the average of the WFE is computed for each half;
4. the differential piston is computed.

In the following plots we show two typical results of such analysis. The left one has been collected in the ATT with the thermal control disabled while the right one inside the LBT dome. The data dispersion is 5 nm and 3 nm respectively.

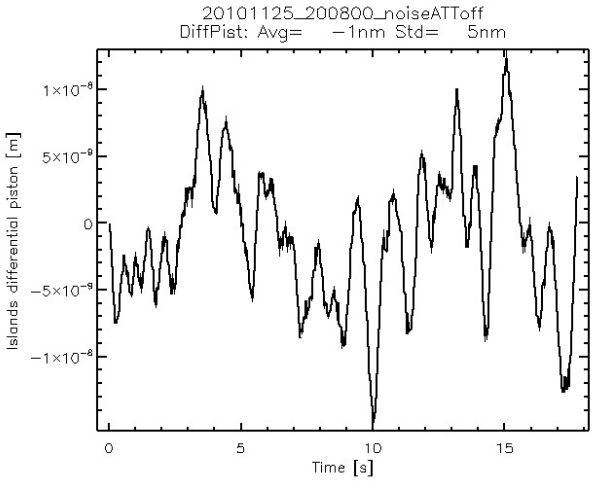

Figure 4. Values of the differential piston as measured by the interferometer on two halves of the LBT adaptive secondary. Data have been collected in the optical test tower in Italy; the ±20 nm spread is due to different convection features over the two halves.

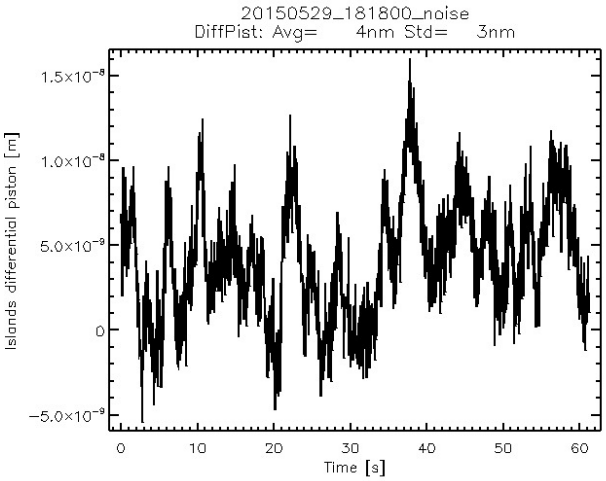

Figure 5. Same analysis on a dataset collected in the LBT telescope dome.

In the current optical configuration the telescope spider is not visible, so that the phase map is not divided by large vignetted gaps. The spatial continuity of the optical surface is then maintained but for the millimiter scale of the inter-segment gaps, thus further helping the identification of the differential piston. Optics manufacturing is responsible for measurement errors due to non zero average WF signal over the segments. To further assess its contribution a detailed budgeting is necessary, including the M3 and M5 manufacturing errors, especially at the low spatial scales (comparable to the segment size).

5. CONCLUSION

We outlined a possible instrument to measure the M4 optical figure at the telescope. The goal is to provide a co-phasing strategy to ensure the long-term (years) stability of the mirror phasing. In order to work properly, the instrument shall also check (and in case perform) the flattening and co-aligning of the mirror, thus delivering in the end a fresh calibration of the M4 unit. We expect that the duration of the pure flattening and phasing procedure takes no more than 30 minutes, while the entire calibration (including the measurement of the IF) may take a couple of hours.
Such risk mitigation approach for the phasing stability provides also some benefits to the E-ELT and M4 system.

- As first, it is a quick monitoring of the adaptive mirror (to be run upon schedule).
- It is a time-efficient, risk-free setup for the fine-tune of the mirror after refurbishment, shell swapping, electronics replacement. It allows in fact to run the full optical calibration procedure without the need to move the unit into the optical test tower, i.e. with no need to dismount it from the telescope.
- It allows the full-aperture measurement of the mirror for a cross-check of the sub-aperture, stitched measurements acquired in the test tower during the initial calibration.

As a next step, we will investigate the single pass option based on a fiber-fed interferometer, offering a lower impact from enviroment vibration and air convection. An internal source could also be exploited as a common tool for E-ELT wavefront sensor units, to help during the initial calibration of the systems.

REFERENCES

[1] Biasi, R., Manetti, M., Andrighettoni, M., Angerer, G., Pescoller, D., Patauner, C., Gallieni, D., Tintori, M., Mantegazza, M., Fumi, P., Lazzarini, P., Briguglio, R., Xompero, M., Pariani, G., Riccardi, A., Vernet, E., Pettazzi, L., Lilley, P., and Cayrel, M., "E-ELT M4 adaptive unit final design and construction: a progress report," in [*Adaptive Optics Systems V*], *Proc. of SPIE* **9909**, 99097Y (July 2016).

[2] Pariani, G., Briguglio, R., Xompero, M., and al., "Optical calibration of the ELT: design, alignment and verification of the interferometric test tower," in [*Proceedings of the Fifth AO4ELT Conference*], (July 2017).

[3] Briguglio, R., Pariani, G., Xompero, M., and al., "Optical calibration of the E-ELT adaptive mirror M4: testing protocol and assessment of the measurement accuracy," in [*Proceedings of the Fifth AO4ELT Conference*], (July 2017).

[4] Xompero, M., Briguglio, R., Pariani, G., and al., "Optical calibration of the ELT: strategy for the optical measurement error estimation," in [*Proceedings of the Fifth AO4ELT Conference*], (July 2017).

[5] Briguglio, R., Pariani, G., Xompero, M., Riccardi, A., Tintori, M., Lazzarini, P., and Spanò, P., "8s, a numerical simulator of the challenging optical calibration of the E-ELT adaptive mirror M4," in [*Adaptive Optics Systems V*], *Proc. of SPIE* **9909**, 99097A (July 2016).

[6] Esposito, S., Busoni, L., Bonaglia, M., and al., "A calibration source for ELT AO systems daytime functional and performance verification," in [*Adaptive Optics Systems VI*], *Proc. of SPIE* **10703** (July 2018).

[7] Millerd, J. E., Brock, N. J., Hayes, J. B., North-Morris, M. B., Novak, M., and Wyant, J. C., "Pixelated phase-mask dynamic interferometer," in [*Interferometry XII: Techniques and Analysis*], Creath, K. and Schmit, J., eds., *Proc. of SPIE* **5531**, 304–314 (Aug. 2004).

[8] Briguglio, R., Xompero, M., Riccardi, A., and al., "Optical calibration of the M4 prototype toward the final unit," in [*Proceedings of the Fourth AO4ELT Conference*], (Nov. 2015).